Analytica Chimica Acta 876 (2015) 77–82

Contents lists available at ScienceDirect

Analytica Chimica Acta

journal homepage: www.elsevier.com/locate/aca

Developing a genetically encoded green fluorescent protein mutant for sensitive light-up fluorescent sensing and cellular imaging of Hg(II)

Tao Jiang [a], Daiping Guo [a], Qian Wang [a], Xin Wu [a], Zhao Li [a], Zhenhua Zheng [b], Boyuan Yin [b], Lin Xia [b], Jixian Tang [b], Wenxin Luo [b], Ningshao Xia [b], Yunbao Jiang [a,*]

[a] Department of Chemistry, College of Chemistry and Chemical Engineering, the MOE Key Laboratory of Analytical Sciences, Xiamen University, Xiamen 361005, China
[b] State Key Laboratory of Molecular Vaccinology and Molecular Diagnostics, National Institute of Diagnostics and Vaccine Development in Infectious Disease, School of Life Science, Xiamen University, Xiamen 361005, China

HIGHLIGHTS

- The GFP chemosensors performed a fluorescence light-up response to Hg(II).
- The underlying mechanism was unveiled as a shift between two ground-state populations of GFP.
- The light-up imaging of Hg(II) in living cells was achieved.

GRAPHICAL ABSTRACT

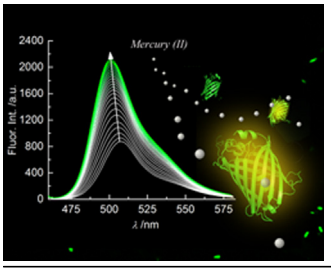

ARTICLE INFO

Article history:
Received 14 February 2015
Received in revised form 16 March 2015
Accepted 18 March 2015
Available online 20 March 2015

Keywords:
Green fluorescent protein-based sensor
Mercury ion
Fluorescence light-up
Cellular imaging

ABSTRACT

Hg(II) is well-known for quenching fluorescence in a distance dependent manner. Nevertheless, when we exposed the fluorophore of a green fluorescent protein (GFP) toward Hg(II), through H148C mutation, the GFP fluorescence could be "lighted up" by Hg(II) down to sub-nM level. The detection linear range is 0.5–3.0 nM for protein solutions at 8.0 nM. The GFPH148C protein displayed a promising selectivity toward Hg(II) and also the cellular imaging capacity. Spectra measurements suggested that the ground-state redistribution of protein contributed to the fluorescence enhancement, which was found not limited to Hg(II), and thus presented an opening for building a pool of GFP-based chemosensors toward other heavy metal ions.

1. Introduction

Hg(II) is an interesting metal ion since it is on one hand toxic, and on the other hand employed in cinnabar (containing HgS) as a traditional Chinese medicine for centuries [1]. It would therefore be of great significance to develop probes that are able to *in vivo* trace Hg(II), for understanding of its toxicity and/or function. Fluorescent chemosensors would naturally be excellent candidates for these purposes, as both high sensitivity and capacity of imaging are possible. Indeed many synthetic fluorescent chemosensors for Hg(II) have been made available [2–5], *e.g.*, chemosensors of organic fluorophores [6–12], oligonucleotide-based sensors [13–17], and protein-based sensors [18]. Some of them exhibit capacity for detection of Hg(II) in living cells or vertebrate organisms. Yet designing single protein-based fluorescent chemosensors would be more demanding since they can be targeted to defined domains of the protein in a noninvasive way, with the expression level controlled by the inducible promoter.

Green fluorescent proteins (GFPs) are, in this regard, ideal candidates because of their stable fluorescence in the absence of

* Corresponding author. Tel.: +86 592 2185662; fax: +86 592 2185662.
E-mail address: ybjiang@xmu.edu.cn (Y. Jiang).

http://dx.doi.org/10.1016/j.aca.2015.03.026
0003-2670/

exogenous cofactors and substrates [19]. Genetically encoded GFP-based chemosensors can be constructed and function with little or reduced influence on the biological and physical properties of most of the host proteins [20–22]. Since the fluorophore in GFP is well protected from the bulky phase by the 11 β-sheet barrel-like structure [23], its accessibility by analytes and hence the sensitivity are reduced. This is probably why GFPs have long been employed as fluorescent labels, whereas relatively limited in terms of single GFP-based fluorescent chemosensors [20–22]. Regarding GFP-based metal ion chemosensors, the enthusiasm has been further dampened, in that heavy metal ions like Hg(II) in the vicinity of the fluorophore is known to quench the fluorescence. Introduction of metal ion binding sites into the fluorescent protein barrel can recapitulate the modes of fluorescent protein metal chemosensors. Introducing histidines, cysteines, or acidic residues [24–30], insertion of metal ion binding peptides or proteins [31–33] have been utilized as strategies to alter the optical property of the single protein in the presence of metal ions. Among them, a Hg(II) quenching chemosensor was reported from the S205C GFP-mutant, with a detection limit of 2 nM [26]. A fluorescence turn-off paper assay was created based on the competitive binding of Hg(II) against the isolated fluorophore toward infrared fluorescent protein [29]. Although turn-off fluorescent sensing dominates thus far, turn-on mode does not have to be precluded. The chromophore imidazole of a blue fluorescent protein mutant BFPms1 was reported to be rigidified by Zn(II), leading to an increase in fluorescence quantum yield [34]. Inserting a copper regulatory protein into yellow fluorescent protein YFP-Ace1 enabled up to 40% fluorescence increasing response toward Cu(I) [33]. Herein we envisaged to construct the GFP fluorescent chemosensors with minimum protein structural distortion. The strategy is to increase exposure of the fluorophore to the bulky solution by mutation of the residues at the "weak" points of the barrel wall. The new amino acid residues would better at the same time afford selectivity toward the analyte. We chose histidine-148 (His148) in the domain of the irregularity of the backbone hydrogen bonds (β-7 to β-8) [35,36]. Since His148 was also reported to protect the chromophore from the solvent and function as the primary acceptor for the protons to the chromophore by donating a hydrogen bond to the phenolic oxygen of the chromophore [37]. Substitution of the imidazole moiety in His148 with a less bulky aliphatic group would create a hole in the β-barrel and enhances the accessibility of the analyte [34,38,39], thereby the photophysics of the chromophore would be influenced more. We established such an access for metal ions to the fluorophore *via* mutation of GFPxm (a variant protein derived from the fluorescent protein of *Aequorea macrodactyla* in the East China Sea [40]) into H148C by replacing the His148 with a cysteine, so that a sulphydryl group was introduced in the close vicinity of the fluorophore, expected to exhibit selective response to the thiophilic Hg(II) ion. We found that the resultant protein did exhibit a highly sensitive light-up fluorescent response towards Hg(II) selectively.

2. Experimental

2.1. Chemicals and materials

Chemicals were purchased from Sinopharm Chem. Reagent (Shanghai, China) or Sangon Biotech. (Shanghai, China), unless otherwise noted. Restriction endonucleases and *Escherichia coli* competent cells BL21 (DE3) were purchased from Promega (Madison, USA). The gel extraction kits were purchased from Watson Biotech. (Shanghai, China). The pTO-T7GFPxm plasmid encoding the sequence of GFPxm was generously provided by Prof. Xia [40]. Metal ions were used as their perchlorates. Alexa Fluor® 488 dye was purchased from Life Tech. (Carlsbad, CA). Lab-Tek® chambered #1.0 borosilicate coverglass was purchased from Sanger Biotech. (Shanghai, China). Water from the Millipore Milli-Q purification system (18 MΩ cm^{-1}) was used throughout experiments.

2.2. Instruments

Fluorescence and absorbance measurements were performed on the Hitachi F4500 fluorescence spectrophotometer, and the Thermo Evolution 300 UV–vis spectrophotometer respectively. Lifetime measurements were performed on the Horiba Fluoromax-4 spectrofluorometer using time-correlated single-photon counting (TCSPC). The pulsed light emitting diode at 455 nm with a repetition rate of 1 MHz and pulse durations <1.5 ns was employed as excitation source. Jasco J-810 spectrometer was employed for circular dichroism (CD) investigation. Fluorescence correlation spectroscopy (FCS) results were obtained from Leica SP5 FCS.

2.3. Protein sensor preparation

Site-directed mutagenesis was introduced by overlap extension polymerase chain reaction (PCR). After verifying the sequence of expression cassette, the mutant cDNA was cloned into the expression vector pTO-T7. The resultant recombinant plasmid was transformed into competent cells of *E. coli* BL21 (DE3). Single colonies were inoculated into LB broth supplemented with kanamycin at 37 °C. When optical density at 600 nm (OD600) reached 0.8, isopropyl β-D-1-thiogalactopyranoside (IPTG) (final concentration 1 mM) was added and cells were further cultured at 22 °C for 6 h. Harvested cells were disrupted through sonication. Protein was first purified by ammonium sulfate precipitation and then ion exchange chromatography on DEAE-Sepharose column (GE). The eluent was collected for further purification *via* 10% native polyacrylamide gel electrophoresis (Native PAGE). Final purity was confirmed by SDS-PAGE and MALDI-MS. Proteins were dialyzed against 5 mM HEPES buffer (pH 7.4), 150 mM NaCl, 1 mM EDTA, 1 mM DTT and concentrated for storage, and buffer exchanged into respective conditions for following measurements. Protein concentration was measured with the Bradford assay.

2.4. Spectroscopic measurements

All measurements were performed under room temperature. Assay of metal ions were performed in 5 mM HEPES buffer (pH 7.4), 150 mM NaCl, unless otherwise noted. Protein samples titrated with Hg(II) were allowed to reach equilibrium for 5 min gentle stirring before measurements. Fluorescein was used as the standard for protein quantum yields measurements. The pH dependence of fluorescence emission was fitted to estimate pK_a using the following equation.

$$F = A + \frac{B}{[1 + 10^{n_H(pK_a - pH)}]} \quad (1)$$

F denotes the fluorescence intensity, A and B are the values of the parameters at acidic and basic pH values. n_H is the Hill coefficient.

For FCS measurements, the 488 nm line of an argon ion laser was used with a 5% of the maximum illumination intensity (*i.e.* 5 mW according to the manufacturer's instructions). The laser was focused by a 1.2 NA/63× water immersion objective onto the sample held in eight-chamber wells with 600 μL $well^{-1}$ and #1.0 borosilicate coverglass. The diameter of pinhole was set to one airy in front of the avalanche photodiode detectors (APD). The acquired $G(\tau)$ was fitted using the ISS VISTA software, according to one component two relaxations function of type [41],

$$G(\tau) = \frac{1}{N}\left[1 + \frac{F}{1-F}\exp\left(\frac{-t}{\tau_C}\right)\right]\frac{1}{[1+(t/\tau_D)]\sqrt{1+\{t/[(Z_0/W_0)^2\tau_D]\}}} \quad (2)$$

N denotes the mean number of fluorescent molecules diffusing in the excitation volume; F is the average fraction of molecules in nonfluorescent state; z_0/w_0 represents the length-to-diameter ratio of the three dimensional Gaussian volume; τ_C and τ_D are the chemical and diffusion relaxation time respectively. In this study, chemical relaxation time means the characteristic relaxation time of dark state in protein. Alexa 488 dye with known diffusion constant was used for calibration, and the value of z_0/w_0 was fitted to be 6.8 with a *ca.* 0.2 fL focal volume.

3. Results and discussion

3.1. Sensor performance

Fluorescence spectrum of the mutant protein was found the same in shape as that of GFPxm (Fig. S1). Mutation, however, changes the absorption spectrum in that the absorbance at 393 nm of the protonated form (form A) of the chromophore increases dramatically at the expense of that of the deprotonated form (form B) (Fig. S2) [42,43]. This change reflects the sensitivity of the chromophore toward the mutation of the surrounding amino acid residues that alter the ionization state of the chromophore in the ground state [44]. Increased pK_a of the mutant H148C (7.44) compared to that of GFPxm (5.74) also suggests the stabilization of form B in H148C (Fig. S3).

A screening of the fluorescent response of H148C and its parent protein GFPxm toward metal ions showed that only with Hg(II), a substantial enhancement in the fluorescence of the mutant H148C by 152 ± 9% was observed by adding 600 nM Hg(II) in 1 μM protein solutions (Figs. 1 and S4). The fluorescence quenching of GFPxm by Cu(II) is also reduced *via* H148C mutation. With the rest of the tested thiophilic metal ions and with GFPxm the fluorescent response is much weaker (<3% quenching). Competitive assays support the selectivity for Hg(II) (Fig. 2), yet partially reduced fluorescence response was observed with Cu(II) and Ag(I) of more than five times the concentration of protein, likely due to the structural disturbance of protein under high metal ion concentrations, and their competitive binding to —SH of 148-cysteine residue in H148C. It is hence confirmed that introducing a cysteine residue at position 148 renders the mutant H148C a selective fluorescent response toward Hg(II).

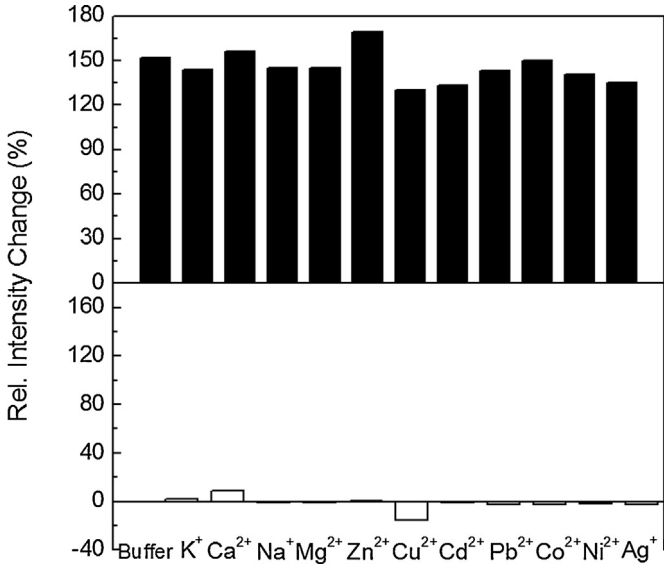

Fig. 2. Changes in the fluorescence intensity of H148C at 1 μM in the presence of competing metal ions in pH 7.4 HEPES buffer. White bar represents the addition of the competing metal ion to the H148C solution at 3 μM of K(I), Ca(II), Na(I), Mg(II), Zn(II), Cd(II), Pb(II), Co(II), Ni(II), and 600 nM of Cu(II) and Ag(I). Black bar represents the co-existence of 600 nM Hg(II) with the respective competitive metal ion mentioned above. Buffer without metal ion was added as the positive control. Ag(I) and Cu(II) at concentration 5 times that of Hg(II), 40–50% of the H148C fluorescence response toward Hg(II) was reduced.

Detailed survey showed that for diluted H148C protein solution at 8 nM, only 0.5 nM Hg(II) could already lead to 12% enhancement in the fluorescence of H148C in buffered solution (Fig. 3), indicating the high sensitivity down to sub-nM level. Excitation spectrum (fluorescence at 508 nm) exhibits a variation profile toward Hg(II) similar to those in the absorption and CD spectra (discussed later), suggesting that Hg(II) populates the "bright" deprotonated form B of H148C even in buffered solutions, that leads to an apparent enhancement in the fluorescence. Adding 2-mercaptoethanol caused fluorescence decrease of H148C mixed with Hg(II) until reaching the starting intensity of H148C. 2-Mercaptoethanol was believed to competitively bind to Hg(II) and take off bound Hg(II) (Fig. S5).

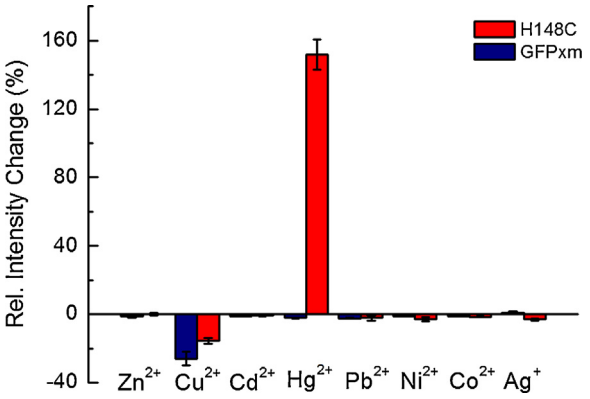

Fig. 1. Change in fluorescence intensity of GFPxm and its mutant H148C at 1 μM as a function of individual metal ions at 600 nM (maximal enhancement for Hg(II)). All measurements were carried out in pH 7.4 HEPES buffer r.t. Error bars represent the standard deviations of three independent measurements.

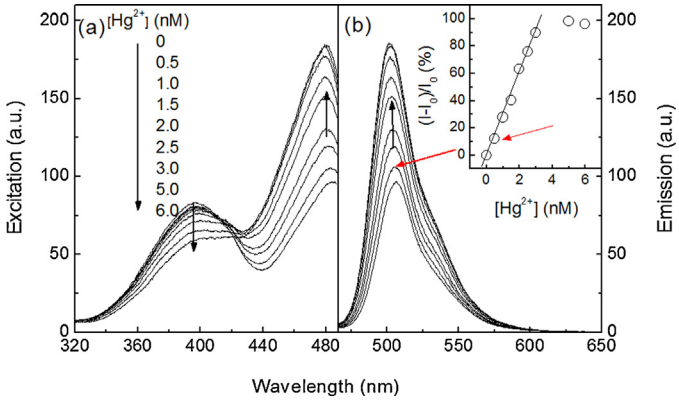

Fig. 3. Detection sensitivity of H148C. (a) Excitation and (b) emission spectra of H148C at 8 nM with varying Hg(II) concentration in pH 7.4 HEPES buffer. Inset in (b) shows change in fluorescence versus [Hg(II)]. Fluorescence spectrum and intensity of H148C with 0.5 nM Hg(II) are indicated by dashed arrows.

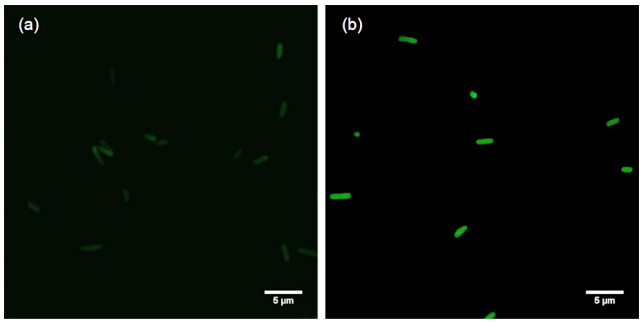

Fig. 4. Confocal fluorescence images of H148C-overexpressing bacteria (a) in the absence of Hg(II), and (b) incubated with 10 μM Hg(II). Samples were excited by 488-nm laser of 1.5 mW.

The capacity in *in vivo* imaging was tested on *E. coli* cells that overexpress the protein (Fig. 4). To quantify the *in vivo* sensing, the fluorescence response of whole cell suspensions toward added Hg (II) was investigated (Fig. S6). Upon incubation with Hg(II), a significant light-up by up to 720%, in the fluorescence relative to that of the untreated cells was observed. Such a higher enhancement in complicated and crowed *in vivo* intracellular environment implies the difference in the process of mercury sensing, which merits further investigation.

3.2. Mechanism investigations

Interaction of Hg(II) with H148C was next investigated for understanding the fluorescence enhancement. Variations in the absorption spectrum of H148C (Fig. 5) suggest that the ground-state populations depends strongly on Hg(II) concentration. After adding up to 30 μM Hg(II) to proteins solutions at 67 μM, the absorbance at 488 nm of form B undergoes a 2-fold increase at the expense of that of form A at 393 nm with an isosbestic point at 420 nm, which indicates a clean ground-state interaction of Hg(II) with H148C. The two corresponding negative peaks in the near-UV range of the CD spectrum of H148C displays a transition profile similar to that seen in the absorption spectrum, suggesting that Hg(II) changes the symmetry of the environment of the chromophore. In the far-UV range (190–240 nm), practically no change in the CD spectrum was induced by Hg(II), implying that Hg(II) does not bring appreciable change in the secondary structure (Fig. S7). In contrast, the absorption spectrum of the parent GFPxm is insensitive to Hg(II) until Hg(II) concentration is 4 times that of the protein, when a transformation of the chromophore form B to form A was identified in a manner opposite to that observed with H148C. Therefore, variation in the H148C fluorescence led by Hg(II) is attributed to the extent to which Hg(II) alters the equilibrium of the two forms (A and B) of the ground-state protein. The introduced cysteine residue at position 148 of H148C appears to facilitate the interaction of Hg(II) with its chromophore within the β-sheet barrel, making the fluorescence of the mutant H148C more sensitive to Hg(II) than that of the parent GFPxm.

Decay of fluorescence at 508 nm of H148C was found to be double exponential, a major component ($f1 = 82\%$) of $\tau_1 = 3.14$ ns and a faster component of $\tau_2 = 0.74$ ns, with an average lifetime of 2.72 ns. The decay heterogeneity is due to multiple excited states, with the faster component relating to the protonated chromophore [45]. At the strongest fluorescence of H148C with of Hg(II), τ_1 decreased to 2.75 ns with a slightly increased $f1$ of 86% while τ_2 increased to 0.85 ns, resulting in a slightly shortened average lifetime (2.48 ns). The quantum yield of form B of the chromophore slightly dropped from 0.74 to 0.67. The light-up fluorescence response of H148C was therefore assigned to the increased population of its bright form in the ground state.

Fluorescence correlation spectroscopy was employed to probe the influence of Hg(II) on the radiationless pathway of H148C by examining the internal photodynamics of single H148C molecules (Figs. 6 and S8). Fig. 6 shows that in the presence of 5 nM Hg(II) when the strongest fluorescence of the protein (8 nM) was observed, an increased population of the nonfluorescent state (the dark state) was observed within the photodynamic time window (<80 μs), from 8 ± 4% without Hg(II) to 20 ± 1%, with a relaxation time of 38 ± 11 μs. This fraction of the dark state was found to rise when the excitation was increased. No aggregation of the protein led by Hg(II) was noted since the fitted diffusion coefficient of H148C remained unchanged. In contrast, fraction of the dark state of GFPxm (18 ± 4%) was found almost the same as that (17 ± 2%) in the presence of 5 nM Hg(II), in agreement with the facts that the fluorescence quantum yield and lifetime of GFPxm are not influenced by Hg(II). The dark state of H148C was proposed to be a triplet-state that was reported to have a relaxation time of *ca.* 30 μs [43]. It hence follows that Hg(II) slightly enhances the transition of the fluorescent protein H148C into dark state,

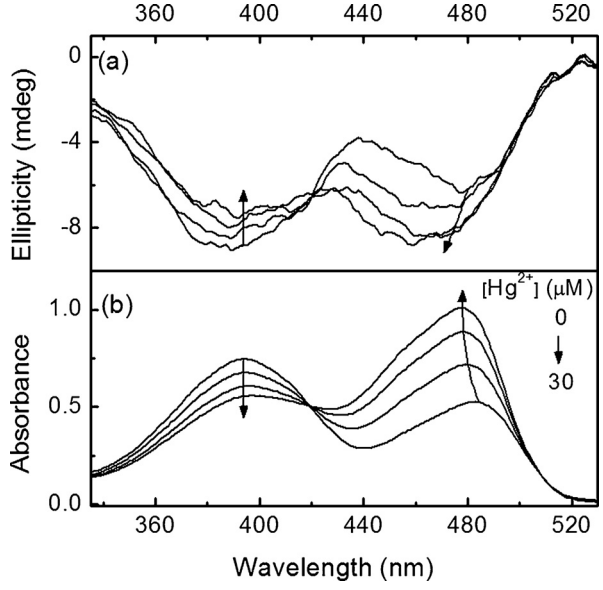

Fig. 5. (a) CD and (b) absorption spectra of H148C at 67 μM with varying Hg(II) concentration (0–30 μM) in pH 7.4 HEPES buffer.

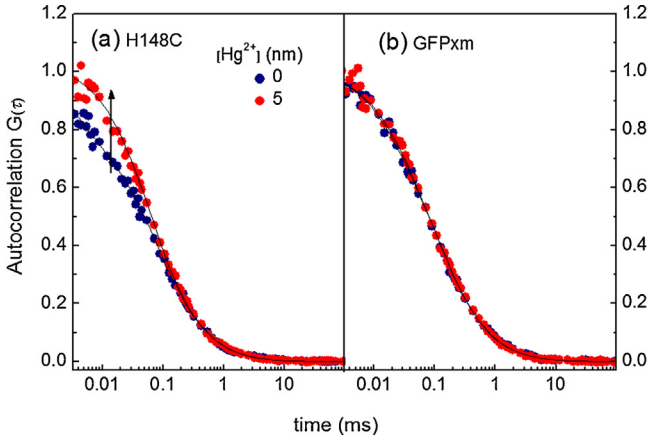

Fig. 6. Normalized autocorrelations $G(\tau)$ of *ca.* 8 nM (a) H148C and (b) GFPxm in the absence and presence of 5 nM Hg(II) in pH 7.4 HEPES buffer at 23 ± 1 °C. Samples were excited by 5 mW 488-nm laser for 10 × 50 s measurements. Fits are given in solid lines.

probably due to its high spin–orbit coupling effect, which explains the minor drops in the lifetime and quantum yield of H148C in the presence of Hg(II).

Identification of Hg(II) binding sites was difficult to deconvolute due to the absence of structural information at atomic-level resolution. We believe there are multiple Hg(II) binding sites on the surfaces of GFP proteins. Based on the data of spectroscopic measurements, we propose that Hg(II) lights up the fluorescence of H148C protein at 148 position on surface, instead of directly coordinating with chromophore. Upon 148 cysteine-Hg(II) binding, Hg(II) probably resembles the parent 148 histidine residue in stabilizing the deprotonated phenoxy of the chromophore, promoting the transformation of chromophore form A to form B.

4. Conclusion

In summary, a rationally designed GFP mutant exhibited a light-up fluorescent response toward Hg(II), with a sub-nM detection limit. The fluorescence enhancement was shown to arise from an increased ground-state population of the deprotonated form that contributes most to the emission of the GFP. Hg(II) is suggested to interact with the chromophore to a higher extent through the access to the cysteine residue that replaces the bulky and chromophore-linked 148-histidine residue. This mechanism involving variation in the ground-state population of the chromophore applies well with our other GFP mutants. For example, Cd(II) can induce the rise of deprotonated form of a H148G mutant (Fig. S9). It is expected that this protocol holds promise for creating GFP-based fluorescent chemosensors sensitive for other heavy metal ions.

Acknowledgments

We thank the support of MOST of China (2011CB910403) and NSFC (91127019, 21275121 and 21435003). The authors declare no competing financial interest.

Appendix A. Supplementary data

Supplementary data associated with this article can be found, in the online version, at http://dx.doi.org/10.1016/j.aca.2015.03.026.

References

[1] E. Ernst, Toxic heavy metals and undeclared drugs in Asian herbal medicines, Trends Pharmacol. Sci. 23 (2002) 136–139.
[2] E.M. Nolan, S.J. Lippard, Tools and tactics for the optical detection of mercuric ion, Chem. Rev. 108 (2008) 3443–3480.
[3] H.N. Kim, W.X. Ren, J.S. Kim, J. Yoon, Fluorescent and colorimetric sensors for detection of lead cadmium, and mercury ions, Chem. Soc. Rev. 41 (2012) 3210–3244.
[4] Y. Yang, Q. Zhao, W. Feng, F. Li, Luminescent chemodosimeters for bioimaging, Chem. Rev. 113 (2013) 192–270.
[5] K.P. Carter, A.M. Young, A.E. Palmer, Fluorescent sensors for measuring metal ions in living systems, Chem. Rev. 114 (2014) 4564–4601.
[6] S. Yoon, A.E. Albers, A.P. Wong, C.J. Chang, Screening mercury levels in fish with a selective fluorescent chemosensor, J. Am. Chem. Soc. 127 (2005) 16030–16031.
[7] S. Yoon, E.W. Miller, Q. He, P.H. Do, C.J. Chang, A bright and specific fluorescent sensor for mercury in water, cells, and tissue, Angew. Chem. Int. Ed. 46 (2007) 6658–6661.
[8] M. Santra, D. Ryu, A. Chatterjee, S.K. Ko, I. Shin, K.H. Ahn, A chemodosimeter approach to fluorescent sensing and imaging of inorganic and methylmercury species, Chem. Commun. (2009) 2115–2117.
[9] A.K. Mandal, M. Suresh, P. Das, E. Suresh, M. Baidya, S.K. Ghosh, A. Das, Recognition of Hg^{2+} ion through restricted imine isomerization: crystallographic evidence and imaging in live cells, Org. Lett. 14 (2012) 2980–2983.
[10] S. Saha, M.U. Chhatbar, P. Mahato, L. Praveen, A.K. Siddhanta, A. Das, Rhodamine–alginate conjugate as self indicating gel beads for efficient detection and scavenging of Hg^{2+} and Cr^{3+} in aqueous media, Chem. Commun. 48 (2012) 1659–1661.
[11] S. Saha, P. Mahato, U. Reddy, G.E. Suresh, A. Chakrabarty, M. Baidya, S.K. Ghosh, A. Das, Recognition of Hg^{2+} and Cr^{3+} in physiological conditions by a rhodamine derivative and its application as a reagent for cell-imaging studies, Inorg. Chem. 51 (2012) 336–345.
[12] U. Reddy G, V. Ramu, S. Roy, N. Taye, S. Chattopadhyay, A. Das, A specific probe for Hg^{2+} to delineate even H^+ in pure aqueous buffer/Hct116 colon cancer cells: Hg(II)-η^2-arene π-interaction and a TBET-based fluorescence response, Chem. Commun. 50 (2014) 14421–14424.
[13] S.V. Wegner, A. Okesli, P. Chen, C. He, Design of an emission ratiometric biosensor from MerR family proteins: a sensitive and selective sensor for Hg^{2+}, J. Am. Chem. Soc. 129 (2007) 3474–3475.
[14] C.K. Chiang, C.C. Huang, C.W. Liu, H.T. Chang, Oligonucleotide-based fluorescence probe for sensitive and selective detection of mercury(II) in aqueous solution, Anal. Chem. 80 (2008) 3716–3721.
[15] D.S. Chan, H.M. Lee, C.M. Che, C.H. Leung, D.L. Ma, A selective oligonucleotide-based luminescent switch-on probe for the detection of nanomolar mercury (II) ion in aqueous solution, Chem. Commun. (2009) 7479–7481.
[16] J. Liu, Y. Lu, Rational design of turn-on allosteric DNAzyme catalytic beacons for aqueous mercury ions with ultrahigh sensitivity and selectivity, Angew. Chem. Int. Ed. 46 (2007) 7587–7590.
[17] J. Zheng, Y. Nie, Y. Hu, J. Li, Y. Li, Y. Jiang, R. Yang, Time-resolved fluorescent detection of Hg^{2+} in a complex environment by conjugating magnetic nanoparticles with a triple-helix molecular switch, Chem. Commun. 49 (2013) 6915–6917.
[18] M. Suresh, S.K. Mishra, S. Mishra, A. Das, The detection of Hg^{2+} by cyanobacteria in aqueous media, Chem. Commun. (2009) 2496–2498.
[19] D.C. Prasher, V.K. Eckenrode, W.W. Ward, F.G. Prendergast, M.J. Cormier, Primary structure of the *Aequorea victoria* green-fluorescent protein, Gene 111 (1992) 229–233.
[20] S.B. Van Engelenburg, A.E. Palmer, Fluorescent sensors of protein function, Curr. Opin. Chem. Biol. 12 (2008) 60–65.
[21] H. Wang, E. Nakata, I. Hamachi, Recent progress in strategies for the creation of protein-based fluorescent biosensors, ChemBioChem 10 (2009) 2560–2577.
[22] A. Ibraheem, R.E. Campbell, Designs and applications of fluorescent protein-based biosensors, Curr. Opin. Chem. Biol. 14 (2010) 30–36.
[23] M. Ormö, A.B. Cubitt, K. Kallio, L.A. Gross, R.Y. Tsien, S.J. Remington, Crystal structure of the *Aequorea victoria* green fluorescent protein, Science 273 (1996) 1392–1395.
[24] T.A. Richmond, T.T. Takahashi, R. Shimkahada, J. Bernsdorf, Engineered metal binding sites on green fluorescence protein, Biochem. Biophys. Res. Commun. 269 (2000) 462–465.
[25] P. Eli, A. Chakrabartty, Variants of DsRed fluorescent protein: development of a copper sensor, Protein Sci. 15 (2006) 2442–2447.
[26] R.R. Chapleau, R. Blomberg, P.C. Ford, M. Sagermann, Design of a highly specific and noninvasive biosensor suitable for real-time in vivo imaging of mercury(II) uptake, Protein Sci. 17 (2008) 614–622.
[27] Y. Rahimi, A. Goulding, S. Shrestha, S. Mirpuri, S.K. Deo, Mechanism of copper induced fluorescence quenching of red fluorescent protein, DsRed, Biochem. Biophys. Res. Commun. 370 (2008) 57–61.
[28] N. Tansila, K. Becker, C. Isarankura Na-Ayudhya, V. Prachayasittikul, L. Bülow, Metal ion accessibility of histidine-modified superfolder green fluorescent protein expressed in *Escherichia coli*, Biotechnol. Lett. 30 (2008) 1391–1396.
[29] Z. Gu, M. Zhao, Y. Sheng, L.A. Bentolila, Y. Tang, Detection of mercury ion by infrared fluorescent protein and its hydrogel-based paper assay, Anal. Chem. 83 (2011) 2324–2329.
[30] E.É. Bálint, J. Petres, M. Szabó, C.K. Orbán, L. Sziláqyi, B. Ábrahám, Fluorescence of a histidine-modified enhanced green fluorescent protein (EGFP) effectively quenched by copper(II) ions, J. Fluoresc. 23 (2013) 273–281.
[31] B. Hötzer, R. Ivanov, S. Altmeier, R. Kappl, G. Jung, Determination of copper(II) ion concentration by lifetime measurements of green fluorescent protein, J. Fluoresc. 21 (2011) 2143–2153.
[32] J. Liang, M. Qin, R. Xu, X. Gao, Y. Shen, Q. Xu, Y. Cao, W. Wang, A genetically encoded copper(I) sensor based on engineered structural distortion of EGFP, Chem. Commun. 48 (2012) 3890–3892.
[33] J. Liu, J. Karpus, S.V. Wegner, P. Chen, C. He, Genetically encoded copper(I) reporters with improved response for use in imaging, J. Am. Chem. Soc. 135 (2013) 3144–3149.
[34] D.P. Barondeau, C.J. Kassmann, J.A. Tainer, E.D. Getzoff, Structural chemistry of a green fluorescent protein Zn biosensor, J. Am. Chem. Soc. 124 (2002) 3522–3524.
[35] G.N. Phillips Jr., Structure and dynamics of green fluorescent protein, Curr. Opin. Struct. Biol. 7 (1997) 821–827.
[36] V. Helms, T.P. Straatsma, J.A. McCammon, Internal dynamics of green fluorescent protein, J. Phys. Chem. B 103 (1999) 3263–3269.
[37] K. Brejc, T.K. Sixma, P.A. Kitts, S.R. Kain, R.Y. Tsien, M. Ormö, S.J. Remington, Structural basis for dual excitation and photoisomerization of the *Aequorea victoria* green fluorescent protein, Proc. Natl. Acad. Sci. U. S. A. 94 (1997) 2306–2311.
[38] R.M. Wachter, M.A. Elsliger, K. Kallio, G.T. Hanson, S.J. Remington, Structural basis of spectral shifts in the yellow-emission variants of green fluorescent protein, Structure 6 (1998) 1267–1277.
[39] R.M. Wachter, R. Yarbrough, K. Kallio, S.J. Remington, Crystallographic and energetic analysis of binding of selected anions to the yellow variants of green fluorescent protein, J. Mol. Biol. 301 (2000) 157–171.
[40] W.X. Luo, T. Cheng, B.Q. Guan, S.W. Li, J. Miao, J. Zhang, N.S. Xia, Variants of green fluorescent protein GFPxm, Mar. Biotechnol. 8 (2006) 560–566.

[41] P. Schwille, S. Kummer, A.A. Heikal, W.E. Moerner, W.W. Webb, Fluorescence correlation spectroscopy reveals fast optical excitation-driven intramolecular dynamics of yellow fluorescent proteins, Proc. Natl. Acad. Sci. U. S. A. 97 (2000) 151–156.
[42] R. Heim, D.C. Prasher, R.Y. Tsien, Wavelength mutations and posttranslational autoxidation of green fluorescent protein, Proc. Natl. Acad. Sci. U. S. A. 91 (1994) 12501–12504.
[43] U. Haupts, S. Maiti, P. Schwille, W.W. Webb, Dynamics of fluorescence fluctuations in green fluorescent protein observed by fluorescence correlation spectroscopy, Proc. Natl. Acad. Sci. U. S. A. 95 (1998) 13573–13578.
[44] A.D. Kummer, J. Wiehler, H. Rehaber, C. Kompa, B. Steipe, M.E. Michel-Beyerle, Effects of threonine 203 replacements on excited-state dynamics and fluorescence properties of the green fluorescent protein (GFP), J. Phys. Chem. B 204 (2000) 4791–4798.
[45] M. Chattoraj, B.A. King, G.U. Bublitz, S.G. Boxer, Ultra-fast excited state dynamics in green fluorescent protein: multiple states and proton transfer, Proc. Natl. Acad. Sci. U. S. A. 93 (1996) 8362–8367.